

# Pd/silica cluster catalysts: synthesis and reactivity with H<sub>2</sub> and C<sub>2</sub>H<sub>4</sub>

Scott N. Reifsnyder and H. Henry Lamb<sup>1</sup>

*Department of Chemical Engineering, North Carolina State University, Box 7905, Raleigh, NC 27695, USA*

Received 1 March 1996; accepted 1 May 1996

Silica-supported Pd clusters were characterized by in situ EXAFS spectroscopy. Clusters with an average nuclearity of six atoms were derived from either an inorganic or an organometallic precursor by reduction at 100–150°C. Despite the small size of the clusters, EXAFS contributions from the metal–support interface were not detected. These clusters and larger ones formed by reduction at 320°C absorb hydrogen on cooling in H<sub>2</sub> to 30°C; the resultant interstitial hydride species decompose in vacuo at 30°C. Vacuum treatment at 300°C removes chemisorbed H<sub>2</sub> yielding bare Pd clusters. In contrast to larger crystallites, the Pd clusters do not react with C<sub>2</sub>H<sub>4</sub> at 150°C to form interstitial carbide species.

**Keywords:** palladium catalysts; metal clusters; EXAFS spectroscopy; hydride; carbide

## 1. Introduction

Supported metal catalysts containing noble metal clusters < 10 Å in size can be prepared using organometallic and inorganic precursors. These supported cluster catalysts often have unique properties which result from geometric and electronic size effects and metal–support interactions [1]. Until now, a systematic investigation of hydride and carbide formation in supported Pd clusters has not been reported.

Bulk Pd readily absorbs hydrogen forming two hydride phases ( $\alpha$  and  $\beta$ ); the maximum hydrogen solubility corresponds to a  $\beta$ -phase stoichiometry of PdH<sub>0.68</sub>. Previous studies have demonstrated hydrogen solubility decreases with Pd crystallite size [2–4]. Boudart and Hwang [2] reported a linear decrease in hydrogen solubility as Pd dispersion increased from 10 to 100%. This result has a simple interpretation: as the fraction of surface atoms increases the number of interstitial sites available for absorbed hydrogen decreases.

Exposure of supported Pd crystallites to ethylene, acetylene, or CO leads to formation of two interstitial carbide phases [5]. Carbide formation from ethylene is facile, occurring at  $\geq 150^\circ\text{C}$ . The maximum carbon concentration is  $\sim 13$  at%. It has been proposed that the carbon atoms occupy the same sites as the hydrogen and, therefore, inhibit hydride formation. McCaulley [6] reported a reduction in the maximum carbon concentration in supported Pd crystallites with decreasing particle size. The presence of the carbide phase has been suggested to inhibit ethylene dehydrogenation and improve vinyl acetate selectivity [7,8].

In this work, Pd/silica cluster catalysts were prepared from an organometallic precursor [Pd( $\eta^5$ -C<sub>5</sub>H<sub>5</sub>)( $\eta^3$ -C<sub>3</sub>H<sub>5</sub>)], [Pd(Cp)(allyl)], and from a conventional metal

salt precursor, [Pd(NH<sub>3</sub>)<sub>4</sub>][NO<sub>3</sub>]<sub>2</sub>. In situ FTIR spectroscopy was used to investigate the chemisorption of [Pd(Cp)(allyl)] on silica. The supported Pd clusters were characterized by in situ EXAFS spectroscopy, and their propensities to form interstitial hydrides and carbides by reaction with H<sub>2</sub> and C<sub>2</sub>H<sub>4</sub> were established.

## 2. Experimental

### 2.1. Catalyst preparation

**General:** Silica (Degussa Aerosil, 300 m<sup>2</sup>/g) was washed with deionized (DI) water and dried in air at 100°C. H<sub>2</sub> and He (UHP grade) were further purified by passage through Altech Oxy-traps and molecular sieve traps. A mixture of 5% C<sub>2</sub>H<sub>4</sub> in N<sub>2</sub> (National Welders) was dried by passage through a molecular sieve trap. [Pd(NH<sub>3</sub>)<sub>4</sub>][NO<sub>3</sub>]<sub>2</sub> (Strem Chemicals) was used as received. [Pd(Cp)(allyl)] was prepared as reported in the literature [9] and was recrystallized from dry hexanes prior to use. Hexanes were dried by distillation from sodium benzophenone ketyl. Air-sensitive samples were stored in nitrogen-filled mBraun gloveboxes.

**Ion exchange:** A 2500 ppm solution of [Pd(NH<sub>3</sub>)<sub>4</sub>][NO<sub>3</sub>]<sub>2</sub> in DI water was added dropwise to a slurry of silica (4 g) in DI water (50 ml). After 24 h, the solid was recovered by filtration, washed with DI water and dried in air at 100°C. The catalyst was calcined by heating at 0.5°C/min to 230°C in flowing extra dry O<sub>2</sub> (600 ml/min); the final calcination temperature was maintained for 2 h. The resultant light-brown catalyst is designated Pd(IE)/silica.

**Organometallic adsorption from solution:** Silica samples (2 g) were calcined in flowing O<sub>2</sub> (600 ml/min) at 250 and 400°C for 2 h. Subsequently, the calcination tube was evacuated by a liquid-N<sub>2</sub>-trapped mechanical

<sup>1</sup> To whom correspondence should be addressed.

pump (base pressure  $10^{-3}$  Torr) for 1 h at the calcination temperature and stored in a glovebox. The resultant supports are designated silica<sub>250</sub> and silica<sub>400</sub>, respectively. [Pd(Cp)(allyl)] (32 mg) was dissolved in dry hexanes (100 ml) forming an orange solution. Calcined silica (1.9 g) was added to the Pd-containing solution under N<sub>2</sub>. After 12 h, the solid was recovered by filtration, yielding a light-brown powder designated as either Pd(CpA)/silica<sub>250</sub> or Pd(CpA)/silica<sub>400</sub> and stored in a glovebox.

**Organometallic vapor adsorption:** A self-supporting wafer of silica<sub>250</sub> was loaded into an in situ FTIR cell under N<sub>2</sub>. The cell was evacuated, and the support was exposed to [Pd(Cp)(allyl)] vapor for 2 h at 30°C. The organometallic precursor was sublimed by heating to 70°C. In subsequent treatments, the cell was evacuated at 100°C for 0.5 h, and the catalyst was exposed to flowing H<sub>2</sub> (100 ml/min) at 100°C for 1 h.

## 2.2. EXAFS spectroscopy

X-ray absorption measurements were made on beamline X-11A of the National Synchrotron Light Source at Brookhaven National Laboratory. The storage-ring energy was 2.5 GeV and the current decayed from 250 to 110 mA during a typical fill. The beamline monochromator was equipped with a pair of Si(111) crystals for operation in the region of the Pd K edge (24350 eV). An Ar-filled ionization chamber was used to measure  $I_0$  and a Kr-filled ionization chamber was used to measure  $I$ .

The Pd/silica catalysts were treated at the beamline in in situ cells [10]. The air-sensitive catalysts derived from [Pd(Cp)(allyl)] were loaded into cells under N<sub>2</sub> in an mBraun glovebox. Catalyst treatments were performed by attaching a cell to a stainless-steel vacuum manifold equipped with an 80  $\ell$ /s turbo pump, a capacitance manometer and a cold cathode gauge. UHP gases passed through H<sub>2</sub>O and O<sub>2</sub> getter traps; the flow rates were controlled by needle valves and monitored using calibrated rotameters. The Pd(CpA)/silica and Pd(IE)/silica catalysts were heated in flowing He (100 ml/min) at 200°C for 0.5 h, cooled to < 50°C, and treated in flowing H<sub>2</sub> at the specified reduction temperature for 1.0 h. Spectra of the freshly reduced catalysts were measured under H<sub>2</sub> at approximately -170°C. After measurements under H<sub>2</sub>, the cell was evacuated at either low (30 or 150°C) or high (300°C) temperature to remove hydrogen from the supported Pd clusters. The cell was subsequently backfilled with He at 30°C and 1 atm prior to EXAFS measurements at -170°C.

Normalized EXAFS spectra were isolated from the experimental data using standard procedures [11]. The EXAFS data were Fourier-filtered ( $1.0 < r < 3.4$  Å) to isolate the first coordination shell. The resultant  $\chi$  function was fitted in  $k$  space using a reference derived from

the EXAFS spectrum of Pd foil measured at liquid-N<sub>2</sub> temperature.

Pd loadings were estimated by comparing the Pd K edge X-ray absorption step to that of a Pd/SiO<sub>2</sub> standard.

## 2.3. FTIR spectroscopy

Infrared spectra were measured using an Analect RFX-65 FTIR spectrometer equipped with a high-sensitivity mercury-cadmium-telluride (MCT) detector. Self-supporting wafers were pressed from approximately 50 mg of powdered catalysts using a 20 mm circular die at 2500 psig. The wafers were loaded into a transmission FTIR spectroscopy cell. The cell consists of a Pyrex tube fitted with o-ring sealed, water-cooled CaF<sub>2</sub> windows and wrapped with electrical heating tape. The cell is attached to a Pyrex vacuum manifold equipped with greaseless stopcocks, an 80  $\ell$ /s turbo pump (base pressure of  $10^{-6}$  Torr), an ion gauge, and capacitance manometers.

## 3. Results and discussion

### 3.1. [Pd(Cp)(allyl)] adsorption on silica

Recently, [Pd(Cp)(allyl)] has been used as a precursor of Pd clusters on MgO and in Y and L zeolites [12,13]. Fig. 1 shows the infrared spectrum of surface species produced by saturation exposure of a silica<sub>250</sub> wafer to [Pd(Cp)(allyl)] vapor at 30°C. The background absorption of the silica<sub>250</sub> wafer has been removed by subtraction. Table 1 summarizes the observed peaks along with reported infrared bands of [Ni(Cp)<sub>2</sub>] [14,15], cyclopentadiene vapor (CpH) [16] and [Pd(allyl)Cl]<sub>2</sub> [17]. The spectrum is consistent with the presence of Pd-Cp moieties (3070, 1635, and 1431 cm<sup>-1</sup>), Pd-allyl moieties (3070, 3040, 1490, 1465, and 1385 cm<sup>-1</sup>), and CpH (3100, 2925, 1635, and 1385 cm<sup>-1</sup>). After evacuation and heating to 100°C, the peaks assigned to Pd-Cp and CpH are diminished. The peaks which remain after this treatment are assigned to Pd-allyl moieties. These peaks are in good agreement with those of [Pd(allyl)Cl]<sub>2</sub>, suggesting the formation of Pd<sup>II</sup>(allyl) surface species. The peaks in the 2850–2980 cm<sup>-1</sup> region, which are assigned to alkane C-H stretching vibrations, have increased in intensity after evacuation.

Fig. 2 shows infrared difference spectra in the OH stretching region that were obtained by subtraction of the silica<sub>250</sub> background. The surface of silica<sub>250</sub> is nearly fully hydroxylated, and infrared bands are observed at 3750 cm<sup>-1</sup> (sharp) and approximately 3550 cm<sup>-1</sup> (broad) owing to isolated and hydrogen-bonded (vicinal) hydroxyl groups, respectively. The negative peaks observed at 3750 and 3725 cm<sup>-1</sup> in fig. 2 are indicative of the consumption of surface hydroxyl groups

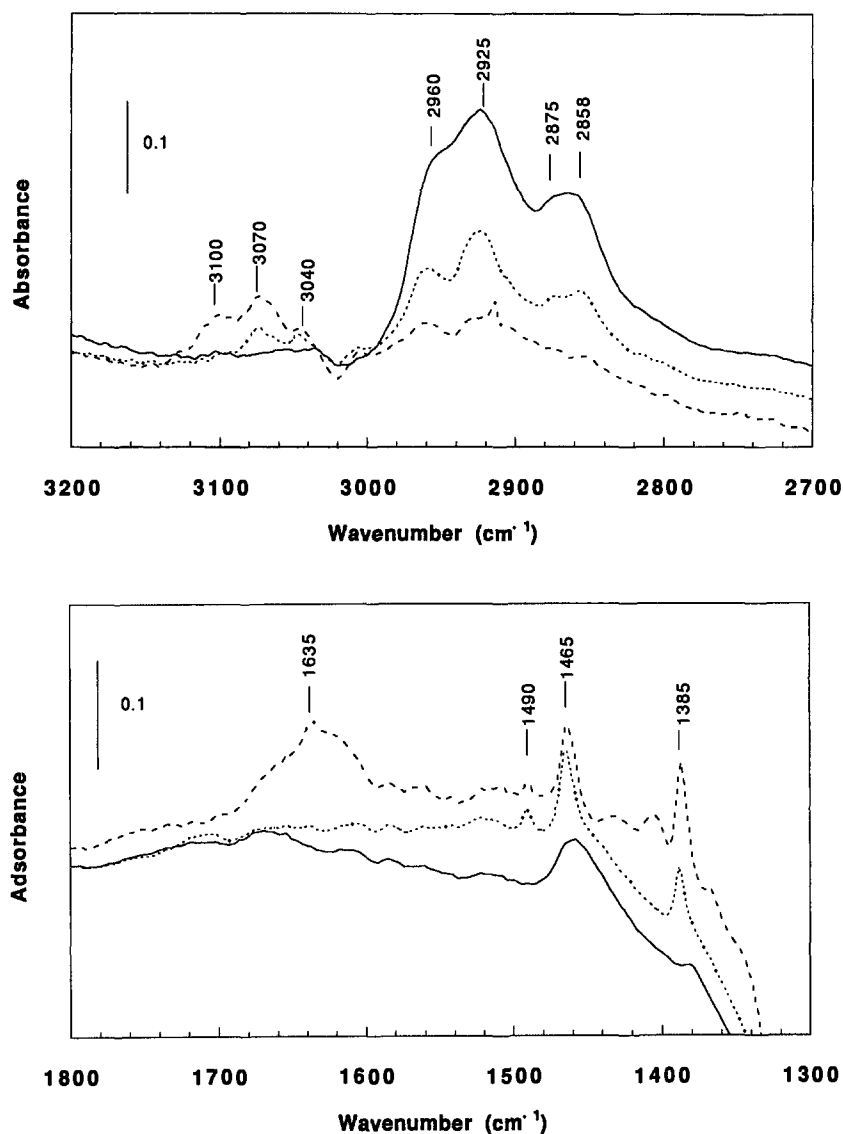


Fig. 1. Infrared difference spectra of surface species on silica<sub>250</sub>: during exposure to [Pd(Cp)(allyl)] vapor at 30°C (dashed line), after subsequent evacuation at 100°C (dotted line), and after subsequent reduction in H<sub>2</sub> at 150°C (solid line).

Table 1  
IR bands of species derived from [Pd(Cp)(allyl)] on silica<sub>250</sub> and reference compounds

	Wavenumbers (cm <sup>-1</sup> )									
<i>sample treatments</i>										
adsorption, 25°C	3100m	3070m	3040w	<sup>a</sup>	1635m	1490w	1465m	1431w	1407w	1385m
evacuation, 100°C		3070w	3040w	<sup>a</sup>	—	1490w	1465m	—	—	1385m
H <sub>2</sub> , 150°C		—	—	<sup>a</sup>	—	—	1465m	—	—	1385w
<i>reference compounds</i>										
Ni(Cp) <sub>2</sub> [14–16]		3075s			1650m			1430m		
CpH [16]	3120s			2935m						1383s
[Pd(allyl)Cl <sub>2</sub> ] [17]		3065w	3030w			1488w	1461s			1385s

<sup>a</sup> CH<sub>3</sub> and CH<sub>2</sub> stretching bands are observed at 2960, 2925, 2875, and 2858 cm<sup>-1</sup>.

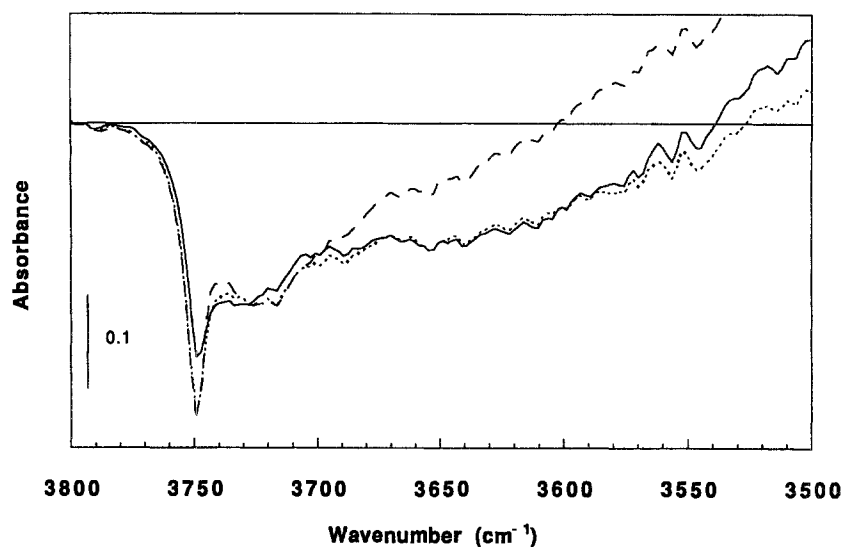
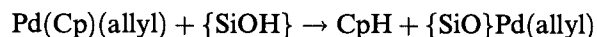


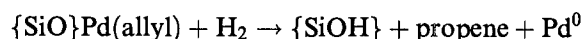
Fig. 2. Infrared difference spectra of silica<sub>250</sub> in the  $\nu_{\text{OH}}$  region: after exposure to [Pd(Cp)(allyl)] vapor at 30°C (dashed line), after subsequent evacuation at 100°C (dotted line), and after subsequent reduction in H<sub>2</sub> at 150°C (solid line).

concomitant with [Pd(Cp)(allyl)] adsorption. Upon evacuation, a broad negative feature near 3600 cm<sup>-1</sup> becomes evident, consistent with consumption of vicinal OH groups.

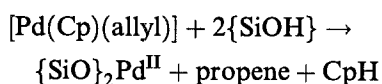
The results indicate that chemisorption of [Pd(Cp)(allyl)] vapor on silica<sub>250</sub> occurs via reaction with surface hydroxyl groups:



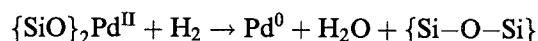
leading to surface-bound Pd<sup>II</sup>(allyl) complexes. (Braces are used to denote species terminating the bulk metal oxide.) We infer that subsequent treatment of [SiOPd(allyl)] in H<sub>2</sub> at 100°C leads to reduction forming propene (or propane) and Pd<sup>0</sup> atoms:



The peaks assigned to [ $\{\text{SiO}\}\text{Pd}(\text{allyl})$ ] decrease markedly in intensity, and the peaks assigned to adsorbed alkanes increase in intensity. Also, the difference spectrum in fig. 2 evidences the regeneration of isolated surface hydroxyl groups; however, recovery of the isolated SiOH absorption is not quantitative. This can be explained if a fraction of the adsorbed Pd was present as Pd<sup>II</sup> oxo species. Consistent with this hypothesis, the infrared spectra of Pd(CpA)/silica<sub>250</sub> and Pd(CpA)/silica<sub>400</sub> catalysts prepared by adsorption of [Pd(Cp)(allyl)] from hexanes solution (with a nominal loading of 0.8 wt% Pd) do not contain peaks characteristic of Pd–Cp or Pd–allyl moieties. We infer that complete protolysis of the Pd–ligand bonds by surface hydroxyl groups occurs at low loadings, resulting in supported Pd<sup>II</sup> oxo species:



Subsequent reduction of the oxo species to Pd<sup>0</sup> would yield water and an Si–O–Si linkage as by-products:



### 3.2. Structures of Pd/silica cluster catalysts

The Pd K edge EXAFS spectrum of Pd(CpA)/silica<sub>400</sub> reduced in H<sub>2</sub> at 100°C (fig. 3a) is characteristic of supported Pd clusters. The Fourier-filtered EXAFS oscillations were fit in  $k$  space ( $6.8 < k < 13.8 \text{ \AA}^{-1}$ ) using a single Pd–Pd shell, and the resultant structural parameters are given in table 2. A comparison of the experimental and calculated  $\chi$  functions in  $k$  space and  $r$  space is shown in fig. 4. A single Pd–Pd shell fits the data well, indicating that any Pd–O or Pd–Si EXAFS contributions associated with the metal–support interface are very weak. Similar EXAFS results were obtained for Pd(CpA)/silica<sub>250</sub> reduced at 100°C and are included in table 2. In both cases, the Pd–Pd coordination number is indicative of an average cluster nuclearity of six atoms, and the Pd–Pd bond distance in the clusters is approximately 1% greater than in bulk Pd (2.75 Å).

For Pd(CpA)/silica<sub>400</sub>, subsequent evacuation of H<sub>2</sub> at 30°C results in a decrease of the Pd–Pd bond distance to 2.76 Å, but has no effect on Pd cluster size (table 2). We infer that Pd hydride clusters were present initially and that removal of the supporting H<sub>2</sub> atmosphere was sufficient to decompose them, leaving clusters covered by chemisorbed hydrogen (*vide infra*). This behavior is analogous to that of 25 Å Pd crystallites supported on carbon and on  $\gamma\text{-Al}_2\text{O}_3$ : the  $\beta\text{-PdH}$  phase decomposes in the absence of H<sub>2</sub> at 30°C [6], whereas, hydrogen adsorbed on the surface of Pd crystallites is stable [18]. In bulk  $\beta\text{-PdH}$ , the hydrogen atoms tend to cluster in the

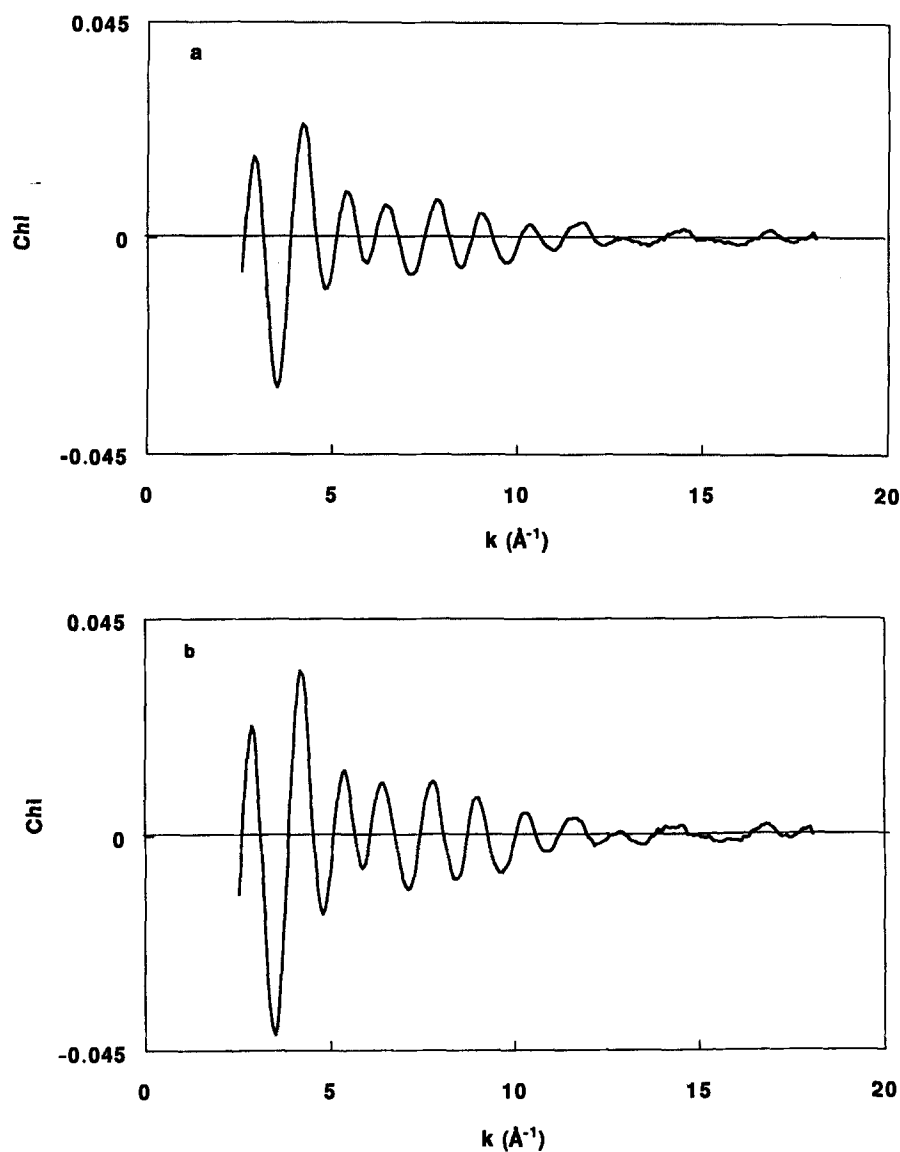


Fig. 3. Pd K edge EXAFS spectra of (a) Pd(CpA)/silica<sub>400</sub> reduced at 100°C and (b) Pd(CpA)/silica<sub>250</sub> reduced at 320°C.

Table 2  
Pd K edge EXAFS results for Pd/silica cluster catalysts

Catalyst description	Pd loading (wt%)	Treatment / temp. (°C)	$N_{\text{Pd-Pd}}^a$	$R_{\text{Pd-Pd}}^b$ (Å)	$(\Delta\sigma^2)$ (Å <sup>2</sup> )	$\Delta E$ (eV)
Pd(CpA)/silica <sub>400</sub>	0.8	H <sub>2</sub> /100	3.8	2.78	0.0048	0.4
		vac/300	4.1	2.76	0.0055	-0.1
Pd(CpA)/silica <sub>250</sub>	0.8	H <sub>2</sub> /100	3.7	2.77	0.0055	4.3
		vac/30 C <sub>2</sub> H <sub>4</sub> /150	— 3.5	— 2.75	— 0.0061	— 7.4
Pd(IE)/silica	0.5	H <sub>2</sub> /150	3.8	2.79	0.0039	0.8
		vac/150	3.6	2.76	0.0045	0.5
Pd(CpA)/silica <sub>250</sub>	0.8	H <sub>2</sub> /320	6.1	2.79	0.0053	0.4
		vac/300	5.8	2.73	0.0045	-0.5

<sup>a</sup> Estimated uncertainty:  $\pm 15\%$ .

<sup>b</sup> Estimated uncertainty:  $\pm 0.01$  Å.

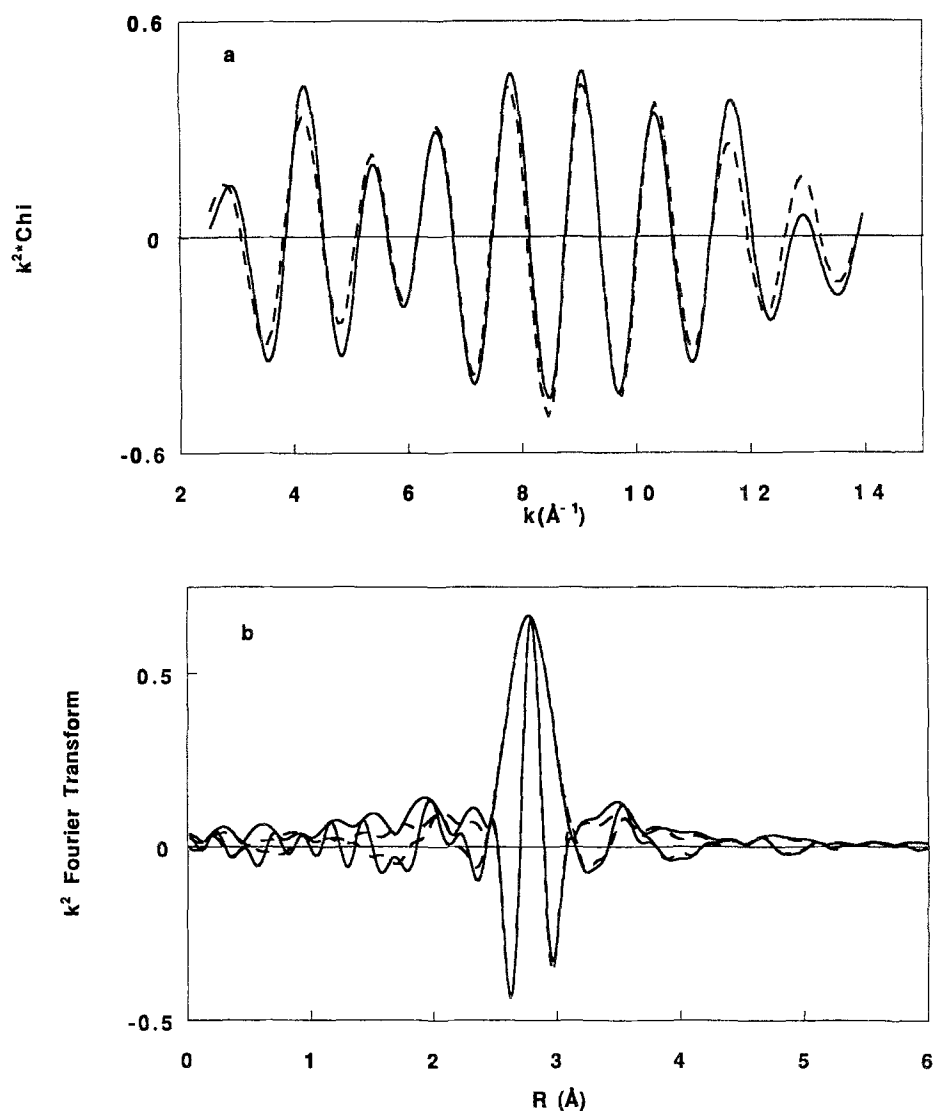


Fig. 4. Comparisons of first-shell Pd K edge EXAFS (solid line) and calculated best fit (dashed line) in  $k$  space and  $r$  space of Pd(CpA)/silica<sub>400</sub> reduced at 100°C: (a)  $k^2$ -weighted  $\chi$  functions, (b)  $k^2$ -weighted Pd-Pd phase-corrected Fourier transforms ( $3.3 < k < 13.8 \text{\AA}^{-1}$ ).

octahedral sites around a central Pd atom; however, at lower concentrations the H atoms are randomly distributed. Although the number of H interstitial sites is restricted in small clusters, the occurrence of interstitial hydride ligands in molecular carbonyl clusters is well-documented [19]. In these molecules, interstitial hydrogen atoms can occupy octahedral, tetrahedral, and square pyramidal sites. With Pd crystallites, a decrease in the relative Debye-Waller factor ( $\Delta\sigma^2$ ) occurs concomitant with decomposition of the  $\beta$ -PdH phase. No corresponding change in Debye-Waller factor is observed with the hydride decomposition in these small Pd clusters.

To test for the formation of Pd carbide clusters, Pd(CpA)/silica<sub>250</sub> (after reduction at 100°C and evacuation at 30°C) was treated in 5% C<sub>2</sub>H<sub>4</sub>/N<sub>2</sub> at 150°C. Similar treatments of palladium black [5] and 25  $\text{\AA}$  supported Pd crystallites [6] result in the formation of a PdC<sub>x</sub> phase with a Pd-Pd bond distance of 2.81  $\text{\AA}$ .

EXAFS analysis of the resultant sample (table 2) evidenced a slight increase in the Debye-Waller factor and a decrease of the Pd-Pd bond distance consistent with the decomposition of the Pd hydride clusters; the supported Pd clusters do not react with C<sub>2</sub>H<sub>4</sub> to form interstitial carbide species under these conditions. We infer that carbide formation is inhibited by a lack of suitable interstitial sites to accommodate carbon atoms.

Reduction of Pd(IE)/silica at 150°C and cooling under H<sub>2</sub> results in the formation of supported Pd hydride clusters that are similar in nuclearity and Pd-Pd bonding to those derived from Pd(CpA)/silica, i.e., the Pd-Pd coordination numbers and bond distances of the samples are equivalent within experimental uncertainty (table 2). The lower relative Debye-Waller factor, however, suggests more ordered structures for the Pd hydride clusters prepared by the conventional ion exchange, O<sub>2</sub> calcination and reduction procedure. We infer from

EXAFS analysis that subsequent heating of Pd(IE)/silica in vacuo at 150°C removes only interstitial hydrogen, as the Pd–Pd distance decreases only to 2.76 Å, which is equivalent to the bulk Pd value. This conclusion is based on analogy to the behavior of small supported Pt clusters for which a significant bond contraction relative to bulk Pt is observed for bare clusters < 10 Å in size [20]. EXAFS studies on supported noble metal clusters of inert supports, like Mylar, also support this expectation [21,22].

Fig. 3b shows the Pd K edge EXAFS spectrum of Pd(CpA)/silica<sub>250</sub> reduced in H<sub>2</sub> at 320°C. The increased EXAFS amplitude in comparison to the spectrum of Pd(CpA)/silica<sub>400</sub> reduced at 100°C (fig. 3a) indicates that, as expected, larger Pd clusters are formed by reduction at higher temperatures. The Fourier-filtered EXAFS oscillations were fitted in *k* space ( $6.8 < k < 13.8 \text{ Å}^{-1}$ ) using a single Pd–Pd shell, and the quantitative results (table 2) demonstrate that although the clusters are larger (containing approximately 20 atoms), the bond distance and disorder are similar to those of Pd hydride clusters produced by low-temperature reduction. As was observed for Pd(CpA)/silica<sub>400</sub> reduced at 100°C, the excellent agreement of the calculated Pd–Pd shell with the experimental data in *k* space and *r* space indicates that EXAFS contributions arising from the metal–support interface are either very weak or absent.

The Pd(CpA)/silica<sub>250</sub> catalyst which was reduced at 320°C was treated subsequently in vacuum at 300°C. The resultant clusters exhibit a 2.2% contraction in the Pd–Pd bond distance relative to the Pd hydride clusters present initially, without a significant change in the Pd–Pd coordination number (table 2). In contrast to the clusters evacuated at 150°C, the Pd–Pd distance is about 1% less than that in bulk Pd. This indicates the loss of surface and interstitial H ligands, yielding bare Pd clusters. The Pd clusters contract, partially compensating for the coordinative unsaturation of the surface atom by an increase in metal–metal bonding.

#### 4. Conclusions

Adsorption of [Pd(Cp)(allyl)] on silica occurs via reaction with surface hydroxyl groups, yielding [{SiO}Pd(allyl)] and [{SiO}<sub>2</sub>Pd] species.

Pd(CpA)/silica<sub>250</sub> and Pd(IE)/silica catalysts contain Pd clusters with an average nuclearity of six atoms after reduction at 150 and 100°C, respectively. Notwithstanding the small cluster size, Pd–O and Pd–Si EXAFS contributions arising from metal–support interfacial bonding were not detected. Pd hydride clusters are formed by cooling in H<sub>2</sub>, and they are decomposed in

vacuo at 30°C. In contrast, treatment of supported Pd clusters in 5% C<sub>2</sub>H<sub>4</sub>/N<sub>2</sub> at 150°C does not result in Pd carbide formation, indicating that the interstitial sites available to hydrogen are inaccessible to carbon. Treatment of Pd clusters in vacuo at 300°C is sufficient to remove absorbed and adsorbed hydrogen; the resultant bare clusters exhibit a 1% contraction of the Pd–Pd bond distance relative to the bulk.

#### Acknowledgement

This work was supported by a grant from Hoechst-Celanese Corporation and an NSF Presidential Young Investigator Award (CTS-8958350). We thank the staff of beamline X-11 of the National Synchrotron Light Source for their assistance.

#### References

- [1] B.C. Gates and D.C. Koningsberger, *CHEMTECH* 22 (1992) 300.
- [2] M. Boudart and H.S. Hwang, *J. Catal.* 39 (1975) 44.
- [3] A.L. Bonivardi and M.A. Baltanas, *J. Catal.* 138 (1992) 500.
- [4] J.A. Eastman, L.J. Thompson and B.J. Kestel, *Phys. Rev. B* 48 (1993) 84.
- [5] S.B. Ziemecki, G.A. Jones, D.G. Swartzfager and R.L. Harlow, *J. Am. Chem. Soc.* 107 (1985) 4547.
- [6] J.A. McCauley, *J. Phys. Chem.* 97 (1993) 10372.
- [7] S.B. Ziemecki and G.A. Jones, *J. Catal.* 95 (1985) 621.
- [8] S.A. Zaidi, *J. Catal.* 68 (1981) 255.
- [9] B.L. Shaw, *Proc. Chem. Soc.* (1960) 247.
- [10] F.W.H. Kampers, T.M.J. Maas, J. van Grondelle, P. Brinkgreve and D.C. Koningsberger, *Rev. Sci. Instr.* 60 (1989) 2635.
- [11] D.E. Sayers and B.A. Bunker, in: *X-Ray Absorption: Principles, Applications, Techniques of EXAFS, SEXAFS, and XANES*, eds. D.C. Koningsberger and R. Prins (Wiley, New York, 1988) p. 211.
- [12] C. Dossi, R. Psaro, A. Bartsch, E. Brivio, A. Galasco and P. Losi, *Catal. Today* 17 (1993) 527.
- [13] C. Dossi, A. Fusi, S. Recchia, M. Anghileri and R. Psaro, *J. Chem. Soc. Chem. Commun.* (1994) 1245.
- [14] G. Wilkinson, P.L. Pauson and F.A. Cotton, *J. Am. Chem. Soc.* 76 (1954) 1970.
- [15] E.R. Lippincott and R.D. Nelson, *Spectrochim. Acta* 10 (1958) 307.
- [16] *Catalog of Infrared Spectral Data*, American Petroleum Institute (1945).
- [17] D.M. Adams and A. Squire, *J. Chem. Soc. A* (1970) 1808.
- [18] P.C. Aben, *J. Catal.* 10 (1968) 224.
- [19] M.D. Vargas and J.N. Nicholls, *Adv. Inorg. Chem. Radiochem.* 30 (1986) 123.
- [20] M. Vaarkamp, *Doctoral Thesis*, Eindhoven University of Technology, The Netherlands (1993).
- [21] A. Balerna, E. Bernieri, P. Picozzi, A. Reale, S. Santucci, E. Burattini and S. Mobilio, *Phys. Rev. B* 31 (1985) 5058.
- [22] G. Apai, J.F. Hamilton, J. Stöhr and A. Thompson, *Phys. Rev. Lett.* 43 (1979) 165.